

An approximate method for solving incompressible Navier-Stokes problem with flow rate conditions *

Alessandro Veneziani, Christian Vergara[†]

Abstract

We consider the incompressible Navier-Stokes problem with flow rate boundary conditions. This problem has been investigated in [2] and [12], following a Lagrange multiplier approach. This approach has the drawback of high computational costs. In this paper, we propose an approximate formulation of the problem, yielding a strong reduction of the computational costs. The error analysis shows that the error introduced by this approximate formulation is confined in a small region of the boundary. This is confirmed by the numerical simulations.

1 Introduction

In many engineering fluid dynamics problem, the computational domain is part of a system or a network. In this case, a part of the boundary does not correspond to a physical wall, and it is just introduced to limit the domain of interest. The prescription of realistic boundary conditions on such *artificial* boundaries can be source of numerical inaccuracies. The problem has been analyzed at the mathematical and numerical levels since about ten years [7]. In particular, in different contexts of internal fluid dynamics there is sometimes the problem of managing numerically *defective boundary data sets*, namely data that are not enough to have a mathematically well posed problem. For instance, it is quite typical in solving fluid problems in a network of pipes like in haemodynamics to have at the inlet only the flow rate. At the practical level, in the engineering literature this problem has been solved by choosing a velocity profile fitting the given flow rate. Since the numerical solution obtained in this way is strongly affected by the selected profile, a common approach is to enlarge the computational domain, in order to reduce the effect of the “arbitrary” profile prescription in the zone of interest. In [7] a different, more mathematically sound, approach is proposed. This is based on finding a suitable variational formulation of the

*This research has been carried out with the support of the EU project “HaeMOdel” and of the Fondazione Politecnico Project “Aneurisk”.

[†]MOX, Department of Mathematics, Politecnico di Milano, 20133 Milano (Italy).
<alessandro.veneziani,christian.vergara@mate.polimi.it

flow rate problem able to include the given data. The defective data set is completed by homogeneous natural boundary condition for the selected variational formulation. This approach can be applied as well to the mean pressure drop problem. In the latter case, it gives very satisfactory results (see e.g. [11]). In the case of flow rate problems, the same approach is somehow problematic at the numerical level, since it requires the definition of non-standard finite dimensional subspaces. A different approach has been therefore proposed in [2]. The basic idea is to consider the flow rate boundary conditions as a constraint for the solution, to be forced through a Lagrange multiplier approach. In this way, we have the drawback of solving an augmented problem, and however the finite dimensional environment for the numerical solution refers to standard functional spaces. This approach has been extensively analyzed in [2] and [12]. The drawback of dealing with an augmented problem is obviously the increment of computational costs. A possible approach relies on splitting the computation of velocity/pressure fields and of the Lagrange multipliers, resorting to a preconditioned Schur complement scheme. The solution of the Navier-Stokes step can be performed with a standard solver [12], however the iterative procedure could be quite expensive in practical applications. In the sequel, we will refer to this approach as *GMRes-based* iterative algorithm, since the solver for the Schur complement problem relies on the well known GMRes method (see for example [10]).

In this work we propose an approximate reformulation of the augmented problem yielding a significant reduction of the computational costs. This reformulation does not imply an iterative approach. The price to pay is the introduction of an error in a small neighborhood of the artificial sections where the flow rate is prescribed. From the practical viewpoint this means that correct numerical results can be obtained in the region of interest by working in a slightly extended computational domain. Even when working with a larger domain, in fact, the computational times of the present method are significantly reduced with respect to the “exact” Lagrange multiplier approach, yielding comparable numerical results in the region of interest. The present proposal could therefore be considered as an intermediate and reliable approach between the engineering one, requiring a relevant expansion of the domain for loosing the effects of the velocity profile selection, and the rigorous one based on the augmented reformulation.

The outline of the work is as follows. We first focus the attention on the linear Stokes problem, by showing how the augmented flow rate problem could be split into three substeps (Sect. 2). The splitting highlights the part of the solution in the augmented problem requiring the highest computational cost. Then, in Section 3 we introduce the approximate splitting, by suitably approximating this step. We will discuss the consistency of the approximate formulation with respect to the exact one and introduce an error analysis of the associated error. The analysis will outline the reduction of the error in the inner part of the computational domain, sufficiently far from the boundary where the flow rates

are prescribed.

In Sect. 4 we present the numerical formulation of the method. In Sect. 5 we consider the possible extensions to the nonlinear Navier-Stokes problem. In particular, we address the case of an implicit time discretization.

Finally, Sect. 6 is devoted to the illustration of several numerical results both from 2D academic and more realistic problems, and for 3D cases of real interest. This research is basically driven by applications in computational haemodynamics (see for example [4]).

2 Different formulations of the flow rate problem

2.1 Basic definitions

Let us consider the domain $\Omega \subset R^d$ ($d = 2, 3$) represented in Fig. 1. We assume that a viscous incompressible fluid flows in Ω . On the boundary denoted by Γ_{wall} we assume that the velocity vanishes (non slip conditions on a rigid boundary). On Γ_{out} we assume homogeneous Neumann conditions, while on Γ_i we assume that the flow rates are prescribed. The problem we are going to consider is therefore (see for example [8]):

$$\begin{cases} \frac{\partial \mathbf{u}}{\partial t} - \mu \Delta \mathbf{u} + \nabla p = \mathbf{f} \\ \nabla \cdot \mathbf{u} = 0 \end{cases} \quad (1)$$

for $\mathbf{x} \in \Omega$ and $t \in (0, T]$, together with the initial condition $\mathbf{u}(\mathbf{x}, 0) = \mathbf{u}_0(\mathbf{x})$ and the boundary conditions:

$$\begin{cases} \mathbf{u} \equiv \mathbf{0} & \text{on } \Gamma_{wall} \\ p\mathbf{n} - \mu \nabla \mathbf{u} \cdot \mathbf{n} = \mathbf{0} & \text{on } \Gamma_{out} \\ \int_{\Gamma_i} \mathbf{u} \cdot \mathbf{n} d\gamma = F_i(t) & \text{for } i = 1, 2, \dots, m. \end{cases} \quad (2)$$

In (1), we denote by $\mathbf{u}(\mathbf{x}, t)$ and $p(\mathbf{x}, t)$ the velocity and pressure field respectively, by μ the fluid viscosity, by F_i the prescribed flow rates as function of time. In particular, in the example of Fig. 1 we have $m = 4$.

This problem is mathematically underdetermined, since the boundary data on Γ_i are not enough to yield well posedness: in fact, three (or two in a 2D problem) scalar data should be prescribed on each point of the boundary, whereas conditions on the flow rates are integral condition over the boundaries Γ_i ($i = 1, 2, \dots, m$). Following [2], we resort to a weak formulation, where the flow rate conditions are considered as a constraint to be imposed with a Lagrange multiplier approach. In particular, problem (1) is weakly formulated as follows (we adopt the standard notation about functional Sobolev spaces): find $\mathbf{u} \in L^2(0, T, \mathbf{H}_{\Gamma_{wall}}^1(\Omega)) \cap L^\infty(0, T, \mathbf{L}^2(\Omega))$ and $p \in L^2(0, T, L^2(\Omega))$ and

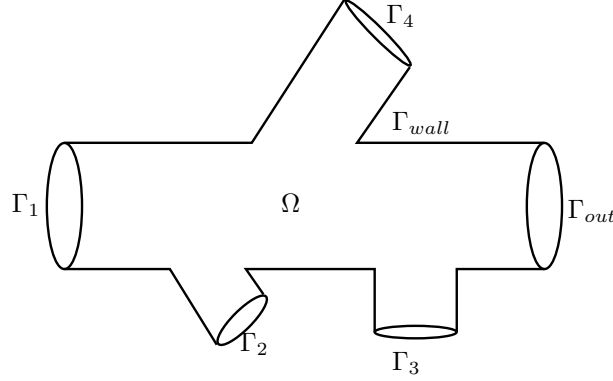


Figure 1: Domain of interest in the flow rate problem.

$\lambda \in (L^2(0, T))^m$ such that for all $\mathbf{v} \in \mathbf{H}_{\Gamma_{wall}}^1(\Omega)$, $q \in L^2(\Omega)$:

$$\begin{cases} \left(\frac{\partial \mathbf{u}}{\partial t}, \mathbf{v} \right) + a(\mathbf{u}, \mathbf{v}) + b(\mathbf{v}, p) + \sum_{i=1}^m \lambda_i \int_{\Gamma_i} \mathbf{v} \cdot \mathbf{n} d\gamma = (\mathbf{f}, \mathbf{v}) \\ b(\mathbf{u}, q) = 0 \\ \int_{\Gamma_i} \mathbf{u} \cdot \mathbf{n} d\gamma = F_i \quad i = 1, 2, \dots, m. \end{cases} \quad (3)$$

where we have set $a(\mathbf{w}, \mathbf{v}) \equiv \int_{\Omega} \mu \nabla \mathbf{w} : \nabla \mathbf{v} d\omega$, $b(\mathbf{v}, q) \equiv \int_{\Omega} \nabla \cdot \mathbf{v} q d\omega$, and

(\cdot, \cdot) denotes the inner product in $\mathbf{L}^2(\Omega)$. The analysis of this problem (and its extension to the nonlinear Navier-Stokes case) has been carried out in [12]. The numerical solution can be achieved by splitting the computation of velocity/pressure from the one of the Lagrange multipliers (GMRes-based algorithm). This approach, that at an algebraic level can be regarded as a *Schur complement method*, at each time step requires $m + 1$ solutions of the Stokes problem having Neumann boundary conditions on Γ_i ($i = 1, 2, \dots, m$). The goal of the present work is to devise an approximate method for solving the problem with a significant reduction of the computational costs.

2.2 An exact splitting

In this Section we introduce a splitting of (3) which is a generalization of the one proposed in [2] for the steady case. More precisely, consider the following subproblems.

1. *Steady Neumann problems.* For all $\mathbf{v} \in \mathbf{H}_{\Gamma_{wall}}^1(\Omega)$, $q \in L^2(\Omega)$, $j =$

$1, 2, \dots, m$ find $\mathbf{w}_j \in \mathbf{H}_{\Gamma_{wall}}^1(\Omega)$, $\pi_j \in L^2(\Omega)$ s.t.

$$\begin{cases} a(\mathbf{w}_j, \mathbf{v}) + b(\mathbf{v}, \pi) = - \int_{\Gamma_j} \mathbf{v} \cdot \mathbf{n} d\gamma \\ b(\mathbf{w}_j, q) = 0 \end{cases} \quad (4)$$

These are m steady problems where natural conditions are prescribed on Γ_i , namely for the j -th problem we impose $p\mathbf{n} - \mu\nabla\mathbf{u} \cdot \mathbf{n}|_{\Gamma_i} = \delta_{ij}\mathbf{n}$ (δ_{ij} is the Kronecker delta).

2. *Unsteady Neumann homogeneous problem.* For all $\mathbf{v} \in \mathbf{H}_{\Gamma_{wall}}^1(\Omega)$, $q \in L^2(\Omega)$, $j = 1, 2, \dots, m$ find $\mathbf{s} \in L^2(0, T, \mathbf{H}_{\Gamma_{wall}}^1(\Omega)) \cap L^\infty(0, T, \mathbf{L}^2(\Omega))$ and $\xi \in L^2(0, T, L^2(\Omega))$ s.t.

$$\begin{cases} \left(\frac{\partial \mathbf{s}}{\partial t}, \mathbf{v} \right) + a(\mathbf{s}, \mathbf{v}) + b(\mathbf{v}, \xi) = (\mathbf{f}, \mathbf{v}) \\ b(\mathbf{s}, q) = 0, \end{cases} \quad (5)$$

with the initial condition $\mathbf{s}(\mathbf{x}, \mathbf{0}) = \mathbf{u}_0$. Note that if $\mathbf{f} = \mathbf{0}$ and $\mathbf{u}_0 = \mathbf{0}$ this problem admits the trivial solution $\mathbf{s} = \mathbf{0}$ and $\xi = 0$. By exploiting this circumstance, numerical solution of (5) can be skipped in this case.

3. *Linear system.* Denote by \mathbf{B} , and \mathbf{S} the $m \times m$ matrix and the vector respectively with elements

$$B_{ij} = \int_{\Gamma_i} \mathbf{w}_j \cdot \mathbf{n} d\gamma, \quad S_i = \int_{\Gamma_i} \mathbf{s} \cdot \mathbf{n} d\gamma.$$

Let us denote with \mathbf{F} the vector with components F_i ($i = 1, \dots, m$). We find therefore the vector $\boldsymbol{\eta}(t)$ by solving

$$\mathbf{B}\boldsymbol{\eta} = \mathbf{F} - \mathbf{S}. \quad (6)$$

4. *Unsteady augmented homogeneous problem.* Find $\mathbf{e} \in L^2(0, T, \mathbf{H}_{\Gamma_{wall}}^1(\Omega)) \cap L^\infty(0, T, \mathbf{L}^2(\Omega))$ and $\varepsilon \in L^2(0, T, L^2(\Omega))$ and $\boldsymbol{\nu} \in (L^2(0, T))^m$ such that for all $\mathbf{v} \in \mathbf{H}_{\Gamma_{wall}}^1(\Omega)$, $q \in L^2(\Omega)$:

$$\begin{cases} \left(\frac{\partial \mathbf{e}}{\partial t}, \mathbf{v} \right) + a(\mathbf{e}, \mathbf{v}) + b(\mathbf{v}, \varepsilon) + \sum_{i=1}^m \nu_i \int_{\Gamma_i} \mathbf{v} \cdot \mathbf{n} d\gamma = - \sum_{j=1}^m \frac{d\eta_j}{dt} (\mathbf{w}_j, \mathbf{v}) \\ b(\mathbf{e}, q) = 0 \\ \int_{\Gamma_i} \mathbf{e} \cdot \mathbf{n} d\gamma = 0 \quad i = 1, 2, \dots, m \end{cases} \quad (7)$$

with the initial condition: $\mathbf{e}(\mathbf{x}, 0) = \mathbf{0}$.

It is possible to verify by linear combination that solution of problem (3) can be written as:

$$\mathbf{u} = \mathbf{s} + \mathbf{e} + \sum_{j=1}^m \eta_j \mathbf{w}_j, \quad p = \xi + \varepsilon + \sum_{j=1}^m \eta_j \pi_j, \quad \lambda_i = \nu_i + \eta_i \quad \forall i = 1, 2, \dots, m.$$

It is worth noting that all the subproblems are well posed under suitable assumptions. Namely, (4) are standard steady Stokes problems, (5) is still a standard unsteady Stokes problem, (7) is a homogeneous augmented problem, analyzed in [2] and [12]. Finally, matrix B in (6) is non singular, as it has been proved in [2]. The steady problems are obviously to be solved once at all at the beginning of computations.

3 The inexact splitting

In the previous splitting, we compute separately the contributions to the solution given by the forcing term and the flow rates. The latter still requires the solution of an augmented (homogeneous) problem, and it is expensive to solve. We therefore approximate problem (7) with the following one. Let us set $\hat{\Gamma} \equiv \Gamma_{wall} \cup \Gamma_1 \cup \dots \cup \Gamma_m \equiv \partial\Omega \setminus \Gamma_{out}$. Find $\hat{\mathbf{e}} \in L^2(0, T, \mathbf{H}_{\hat{\Gamma}}^1(\Omega)) \cap L^\infty(0, T, \mathbf{L}^2(\Omega))$ and $\hat{\varepsilon} \in L^2(0, T, L^2(\Omega))$ such that for all $\mathbf{v} \in \mathbf{H}_{\hat{\Gamma}}^1(\Omega)$, $q \in L^2(\Omega)$:

$$\begin{cases} \left(\frac{\partial \hat{\mathbf{e}}}{\partial t}, \mathbf{v} \right) + a(\hat{\mathbf{e}}, \mathbf{v}) + b(\mathbf{v}, \hat{\varepsilon}) = - \sum_{j=1}^m \frac{d\eta_j}{dt} (\mathbf{w}_j, \mathbf{v}) \\ b(\hat{\mathbf{e}}, q) = 0 \end{cases} \quad (8)$$

with the initial condition: $\hat{\mathbf{e}}(\mathbf{x}, 0) = \mathbf{0}$. This is a standard Stokes problem with homogeneous Dirichlet conditions on $\hat{\Gamma}$.

The outline of the scheme is the following:

1. *Preliminary computations:* Solve the m steady problems (4).
2. *Time loop:* Solve with some numerical time advancing scheme the sequence of (standard) problems (5), (6) and (8).
3. *Final assembling:* Set:

$$\hat{\mathbf{u}} = \mathbf{s} + \hat{\mathbf{e}} + \sum_{j=1}^m \eta_j \mathbf{w}_j, \quad \hat{p} = \xi + \hat{\varepsilon} + \sum_{j=1}^m \eta_j \pi_j. \quad (9)$$

We point out that in this approximation the Lagrange multipliers λ_i are not explicitly computed. Typically, this is not a problem, since the interest is for the velocity and pressure fields. However, in the present variational formulation the Lagrangian multiplier has the physical meaning of the normal stresses (see [11], [2]) and this can be of some interest in the geometrical multiscale

approach proposed in [1], [3] and [5] for coupling 3D models to 1D or lumped parameters models in the framework of computational haemodynamics. In the approximate scheme, the Lagrangian multipliers can be therefore computed as a post-processing step starting from the approximate velocity and pressure fields.

Remark 3.1 *Observe that in the steady case, namely for $\frac{d\eta_j}{dt} = 0$ for each $j = 1, 2, \dots, m$, problem (7) and (8) both have the unique solution $\mathbf{e} = \hat{\mathbf{e}} = \mathbf{0}$. In this case, therefore, the splitting yields the exact solution. Actually, this argument has been exploited in [2], which has inspired the present one, where the decomposition for the steady solution is adopted as a constructive argument for proving the well posedness of the augmented problem.*

3.1 Error analysis

The inexact splitting introduces an error at the fourth subproblem, in solving a standard homogeneous Dirichlet problem replacing the augmented one. This error affects the solution independently of the discretization of the problem: the aim of this section is to prove that this consistency error is confined in a boundary layer in the neighborhood of the sections Γ_j . In fact, since the difference between the exact and inexact schemes is only in solving the fourth subproblem, we compare the solutions of these problems, namely \mathbf{e} and $\hat{\mathbf{e}}$.

In the sequel, the subscript *div* for a functional space will denote the divergence free subspace of the vectors belonging to that space. Actually, we will develop our analysis in divergence free subspaces, so that we will not deal with the pressure field. In particular, we will set $V \equiv \mathbf{H}_{\Gamma_{wall}}^1(\Omega)$ and consequently the divergence free subspace of V will be denoted by V_{div} . For the sake of simplicity, we will refer to the case $m = 1$ and we will denote by Γ the part of the boundary where the flow rate condition is prescribed.

In the divergence free subspace, the fourth problem to be solved in the exact splitting reads: find $\mathbf{e} \in L^2(0, T, V_{div}) \cap L^\infty(0, T, \mathbf{L}^2(\Omega))$ and $\nu \in L^2(0, T)$ such that for all $\mathbf{v} \in V_{div}$:

$$\begin{cases} \left(\frac{\partial \mathbf{e}}{\partial t}, \mathbf{v} \right) + a(\mathbf{e}, \mathbf{v}) + \nu \int_{\Gamma} \mathbf{v} \cdot \mathbf{n} d\gamma = -\frac{d\eta}{dt}(\mathbf{w}, \mathbf{v}) \\ \int_{\Gamma} \mathbf{e} \cdot \mathbf{n} d\gamma = 0 \end{cases} \quad (10)$$

with $\mathbf{e}(\mathbf{x}, 0) = \mathbf{0}$.

Correspondingly, the fourth subproblem in the inexact splitting scheme can be reformulated as follows. Find $\hat{\mathbf{e}} \in L^2(0, T, \mathbf{H}_{\Gamma, div}^1(\Omega)) \cap L^\infty(0, T, \mathbf{L}^2(\Omega))$ such that for all $\mathbf{v} \in \mathbf{H}_{\Gamma, div}^1(\Omega)$:

$$\left(\frac{\partial \hat{\mathbf{e}}}{\partial t}, \mathbf{v} \right) + a(\hat{\mathbf{e}}, \mathbf{v}) = -\frac{d\eta}{dt}(\mathbf{w}, \mathbf{v}) \quad (11)$$

with the initial condition: $\hat{\mathbf{e}}(\mathbf{x}, 0) = \mathbf{0}$.

In order to compare the two solutions, we reformulate the latter problem in a different way.

Lemma 3.1 *Problem (11) is equivalent to the following “augmented” problem: find $\hat{\mathbf{e}} \in L^2(0, T, V_{div}) \cap L^\infty(0, T, \mathbf{L}^2(\Omega))$ and $\zeta \in L^2(0, T, H^{-1/2}(\Gamma))$ such that for all $\mathbf{v} \in V_{div}$ and $\chi \in H^{-1/2}(\Gamma)$:*

$$\begin{cases} \left(\frac{\partial \hat{\mathbf{e}}}{\partial t}, \mathbf{v} \right) + a(\hat{\mathbf{e}}, \mathbf{v}) + \int_{\Gamma} \zeta \mathbf{v} d\gamma = -\frac{d\eta}{dt}(\mathbf{w}, \mathbf{v}) \\ \int_{\Gamma} \chi \hat{\mathbf{e}} d\gamma = 0 \end{cases} \quad (12)$$

with $\hat{\mathbf{e}}(\mathbf{x}, 0) = \mathbf{0}$.

PROOF

The implication that the solution $\hat{\mathbf{e}}$ of (12) solves also (11) is trivial, since it is enough to select in (12) the test functions belonging to $\mathbf{H}_{\Gamma, div}^1$. The opposite implication can be proved, referring e.g. to Lemma 4.1 in [6], by showing that the following inequality holds: there exists a $\beta > 0$ such that for each $\chi \in H^{-1/2}(\Gamma)$ there exists a vector \mathbf{v} such that

$$\int_{\Gamma} \chi \mathbf{v} d\gamma \geq \beta \|\chi\|_{H^{-1/2}(\Gamma)} \|\mathbf{v}\|_V.$$

This inequality holds in consequence of the definition of norm in $H^{-1/2}(\Gamma)$ and of the boundness of the lifting operator from $H^{-1/2}(\Gamma)$ to $\mathbf{H}^1(\Omega)$. \diamond

In the sequel C_k ($k = 1, 2, \dots$) will denote a generic function of time or a constant dependent on the data (but independent of the space coordinate). Observe that as a consequence of the previous Lemma, by standard arguments we have that for $t > 0$

$$\int_0^t \|\zeta\|_{H^{-1/2}(\Gamma)}^2 ds \leq C_1.$$

The error analysis can be now carried out by considering the field $\boldsymbol{\delta} = \mathbf{e} - \hat{\mathbf{e}}$. By subtracting (10) and (12) we have that for all $\mathbf{v} \in V_{div}$

$$\begin{cases} \left(\frac{\partial \boldsymbol{\delta}}{\partial t}, \mathbf{v} \right) + a(\boldsymbol{\delta}, \mathbf{v}) + \int_{\Gamma} (\nu - \zeta) \mathbf{v} \cdot \mathbf{n} d\gamma - \int_{\Gamma} \zeta \mathbf{v} \times \mathbf{n} d\gamma = 0 \\ \int_{\Gamma} \boldsymbol{\delta} \cdot \mathbf{n} d\gamma = 0 \end{cases} \quad (13)$$

with $\boldsymbol{\delta}(\mathbf{x}, 0) = \mathbf{0}$.

We prove the following result.

Theorem 3.2 *Let $\Omega' \subset\subset \Omega$ be such that $\text{dist}(\Omega', \Gamma) \geq \bar{d}$. If the domain Ω is smooth enough, the following inequalities hold for $t > 0$*

$$\begin{cases} \|\boldsymbol{\delta}\|_{\mathbf{L}^2(\Omega)}^2(t) + \alpha \int_0^t \|\boldsymbol{\delta}\|_V^2 \leq C_2 \int_0^t \|\zeta\|_{H^{-1/2}(\Gamma)}, \\ \int_0^t \|\boldsymbol{\delta}\|_{\mathbf{H}^1(\Omega')}^2 \leq C(t, \zeta, \Gamma) e^{-\bar{d}}. \end{cases} \quad (14)$$

PROOF

Let us set in (13) $\mathbf{v} = \boldsymbol{\delta}$. Since ν is constant in space, we obtain

$$\left(\frac{\partial \boldsymbol{\delta}}{\partial t}, \boldsymbol{\delta} \right) + a(\boldsymbol{\delta}, \boldsymbol{\delta}) - \int_{\Gamma} \zeta \boldsymbol{\delta} d\gamma = 0. \quad (15)$$

From the coercivity of the bilinear form $a(\cdot, \cdot)$, we have

$$\frac{1}{2} \frac{d}{dt} \|\boldsymbol{\delta}\|_{\mathbf{L}^2(\Omega)}^2 + \alpha \|\boldsymbol{\delta}\|_V^2 \leq \left| \int_{\Gamma} \zeta \boldsymbol{\delta} d\gamma \right|. \quad (16)$$

Observe that in the special case $\mathbf{e} = \mathbf{0}$ on Γ , we obviously get $\boldsymbol{\delta} = \mathbf{0}$ in the whole Ω as expected. More in general, from this inequality we obtain the first of (14) by integrating in time and applying the Young and the trace inequalities in a standard way.

Let us prove the second (14). The basic approach is similar to the one followed by Rannacher in the analysis of Chorin-Temam method for Navier-Stokes equations, presented in [9]. Let us denote by $d(\mathbf{x})$ the distance of the generic point of the domain Ω from Γ and set $\sigma(\mathbf{x}) \equiv \min(e^{d(\mathbf{x})}, e^{\bar{d}})$. We have:

$$\mu \int_0^t \int_{\Omega'} \nabla \boldsymbol{\delta} : \nabla \boldsymbol{\delta} d\omega ds \leq e^{-\bar{d}} \mu \int_0^t \int_{\Omega} \sigma \nabla \boldsymbol{\delta} : \nabla \boldsymbol{\delta} d\omega ds \leq e^{-\bar{d}} C_4 \int_0^t \|\boldsymbol{\delta} \sqrt{\sigma}\|_V^2 ds. \quad (17)$$

Now, choose $\mathbf{v} = \sigma \boldsymbol{\delta}$ in (13). Since on Γ we have that $\sigma = 1$, $\nu \int_{\Gamma} \sigma \boldsymbol{\delta} = \nu \int_{\Gamma} \boldsymbol{\delta} = 0$

and we have:

$$\frac{1}{2} \frac{d}{dt} \|\boldsymbol{\delta} \sqrt{\sigma}\|_{\mathbf{L}^2(\Omega)}^2 + \mu \int_{\Omega} \nabla \boldsymbol{\delta} : \nabla \boldsymbol{\delta} \cdot \sigma d\omega = -\mu \int_{\Omega} \boldsymbol{\delta} \cdot \nabla \boldsymbol{\delta} \cdot \nabla \sigma d\omega + \int_{\Gamma} \zeta \boldsymbol{\delta} d\gamma. \quad (18)$$

If d is smooth enough, observing that on Ω' we have $\nabla \sigma = 0$ and that on $\Omega \setminus \Omega'$ we have $\nabla \sigma = \sigma \nabla d$, we obtain from the Young inequality:

$$\left| \mu \int_{\Omega} \boldsymbol{\delta} \cdot \nabla \boldsymbol{\delta} \cdot \nabla \sigma d\omega \right| \leq \mu \|\nabla d\|_{L^\infty(\Omega)} \|\boldsymbol{\delta} \sqrt{\sigma}\|_{\mathbf{L}^2(\Omega)} \|\nabla \boldsymbol{\delta} \sqrt{\sigma}\|_{\mathbf{L}^2(\Omega)} \leq$$

$$\leq C_5 \|\delta\sqrt{\sigma}\|_{\mathbf{L}^2(\Omega)}^2 + \mu \|\nabla\delta\sqrt{\sigma}\|_{\mathbf{L}^2(\Omega)}^2.$$

By time integration of (18) and application of the Gronwall Lemma, we obtain:

$$\|\delta\sqrt{\sigma}\|_{\mathbf{L}^2(\Omega)}^2 \leq \int_0^t \|\zeta\|_{H^{-1/2}(\Gamma)}^2 ds e^{C_5 t},$$

yielding

$$\int_0^t \|\delta\sqrt{\sigma}\|_V^2 \leq C(\zeta, |\Gamma|, t)$$

where $C(\zeta, |\Gamma|, t) = \int_0^t \|\zeta\|_{H^{-1/2}(\Gamma)}^2 ds + \int_0^t \int_0^\tau \|\zeta\|_{H^{-1/2}(\Gamma)}^2 d\tau e^{C_5 s} ds$ is increasing with t and $|\Gamma|$. From (17) we finally obtain:

$$\mu \int_0^t \int_{\Omega'} \nabla\delta : \nabla\delta d\omega ds \leq e^{-\bar{d}} C_4 C(\zeta, |\Gamma|, t)$$

yielding the thesis. \diamond

The relevance of the previous result is that at each fixed instant the error in a domain contained in Ω decreases exponentially with the distance from Γ . From the practical viewpoint this implies that the domain of interest can be slightly extended yielding accurate results with a small increase in computational costs. Numerical results confirm this circumstance. In particular, in computational haemodynamics, when following the common approach of prescribing an arbitrary velocity profile fitting the given flow rates one has to extend the vascular district at hand for 3 or 4 diameters of the vessel. Conversely, as we will see, in the present case the expansion of the domain can be limited to a small zone around Γ .

4 Discretization of the inexact splitting

We consider the numerical discretization of the inexact splitting. In particular, we refer to a Galerkin finite element discretization for the space variables and a finite difference time discretization. For the sake of simplicity, we adopt an implicit Euler scheme. More accurate time discretization methods can be considered as well. Let us denote by V_h a finite dimensional subspace of $\mathbf{H}_{\Gamma_{wall}}^1$, for instance given by the piecewise polynomials on a suitable mesh \mathcal{T}_h of the domain. Similarly, let \hat{V}_h be a finite dimensional subspace of $\mathbf{H}_{\hat{\Gamma}}^1$, given by (the same) piecewise polynomial functions. Moreover, let Q_h be a finite dimensional subspace of $L^2(\Omega)$. We suppose that the couples V_h, Q_h and \hat{V}_h, Q_h are *LBB condition* compatible. We denote by Δt a given time step. A possible discrete formulation of the inexact splitting problem is the following.

1. For all $\mathbf{v}_h \in V_h$, $q_h \in Q_h$, $j = 1, 2, \dots, m$ find $\mathbf{w}_{j,h} \in V_h$, $\pi_{j,h} \in Q_h$ s.t.:

$$\begin{cases} a(\mathbf{w}_{j,h}, \mathbf{v}_h) + b(\mathbf{v}_h, \pi_{j,h}) = - \int_{\Gamma_j} \mathbf{v}_h \cdot \mathbf{n} d\gamma \\ b(\mathbf{w}_{j,h}, q_h) = 0 \end{cases} \quad (19)$$

for $j = 1, 2, \dots, m$.

2. At each time step, given the solution at time $t^n = t_0 + n\Delta t$, we solve the following problems. For all $\mathbf{v}_h \in V_h$, $q_h \in Q_h$, find $\mathbf{s}_h^{n+1} \in V_h$ and $\xi_h^{n+1} \in Q_h$ s.t.

$$\begin{cases} \left(\frac{\mathbf{s}_h^{n+1} - \mathbf{s}_h^n}{\Delta t}, \mathbf{v}_h \right) + a(\mathbf{s}_h^{n+1}, \mathbf{v}_h) + b(\mathbf{v}_h, \xi_h^{n+1}) = (\mathbf{f}^{n+1}, \mathbf{v}_h) \\ b(\mathbf{s}_h^{n+1}, q) = 0, \end{cases} \quad (20)$$

with the initial condition $\mathbf{s}_h^0 = \mathbf{u}_{0,h}$, suitable approximation of the initial condition \mathbf{u}_0 and where $\mathbf{f}^{n+1} = \mathbf{f}(t^{n+1})$.

3. Solve the linear system:

$$\mathbf{B}\boldsymbol{\eta}^{n+1} = \mathbf{F}^{n+1} - \mathbf{S}^{n+1}. \quad (21)$$

4. Find $\hat{\mathbf{e}}_h^{n+1} \in \hat{V}_h$ and $\hat{\xi}_h^{n+1} \in Q_h$ such that for all $\mathbf{v}_h \in \hat{V}_h$, $q_h \in Q_h$:

$$\begin{cases} \left(\frac{\hat{\mathbf{e}}_h^{n+1} - \hat{\mathbf{e}}_h^n}{\Delta t}, \mathbf{v}_h \right) + a(\hat{\mathbf{e}}_h^{n+1}, \mathbf{v}_h) + b(\mathbf{v}_h, \hat{\xi}_h^{n+1}) = \\ = - \sum_{j=1}^m \frac{\eta_j^{n+1} - \eta_j^n}{\Delta t} (\mathbf{w}_{j,h}, \mathbf{v}_h) \\ b(\hat{\mathbf{e}}_h^{n+1}, q_h) = 0 \end{cases} \quad (22)$$

with the initial condition: $\hat{\mathbf{e}}_h^0 = \mathbf{0}$.

5 Extension to the Navier-Stokes problem

Our proposal is based on a linear combination of different components of the solution so the linearity of the problem is a key-factor. However, the interest for this kind of problems comes from fields such as the computational haemodynamics, where the nonlinear convective term of the Navier-Stokes equations cannot be dropped out. It is therefore worth addressing a possible extensions of our proposal to the nonlinear case.

Let us start by observing that the extension to the Oseen linear problem:

$$\begin{cases} \frac{\partial \mathbf{u}}{\partial t} + (\boldsymbol{\beta} \cdot \nabla) \mathbf{u} - \mu \Delta \mathbf{u} + \nabla p = \mathbf{f} \\ \nabla \cdot \mathbf{u} = 0 \end{cases} \quad (23)$$

with $\boldsymbol{\beta}$ assigned convective field, is quite straightforward. As a matter of fact, observe that the solution of the flow rate Oseen problem can be obtained following the splitting proposed for the Stokes problem, where equations (4) and (6) are unchanged, while (5) and (7) (or (8) in the inexact splitting) are respectively replaced by:

$$\begin{cases} \left(\frac{\partial \mathbf{s}}{\partial t}, \mathbf{v} \right) + ((\boldsymbol{\beta} \cdot \nabla) \mathbf{s}, \mathbf{v}) + a(\mathbf{s}, \mathbf{v}) + b(\mathbf{v}, \xi) = (\mathbf{f}, \mathbf{v}) \\ b(\mathbf{s}, q) = 0, \end{cases} \quad (24)$$

and

$$\begin{cases} \left(\frac{\partial \mathbf{e}}{\partial t}, \mathbf{v} \right) + ((\boldsymbol{\beta} \cdot \nabla) \mathbf{e}, \mathbf{v}) + a(\mathbf{e}, \mathbf{v}) + b(\mathbf{v}, \varepsilon) + \sum_{i=1}^m \nu_i \int_{\Gamma_i} \mathbf{v} \cdot \mathbf{n} d\gamma = \\ = - \sum_{j=1}^m \frac{d\eta_j}{dt} (\mathbf{w}_j, \mathbf{v}) - \sum_{j=1}^m \eta_j ((\boldsymbol{\beta} \cdot \nabla) \mathbf{w}_j, \mathbf{v}) \\ b(\mathbf{e}, q) = 0 \\ \int_{\Gamma_i} \mathbf{e} \cdot \mathbf{n} d\gamma = 0 \quad i = 1, 2, \dots, m \end{cases}, \quad (25)$$

respectively. Therefore, if the time discretization adopted for solving the Navier-Stokes problem is carried out in an explicit or semi-implicit way, yielding at each time step a Stokes or an Oseen problem, in which $\boldsymbol{\beta}$ is a suitable function of the velocity computed before the current instant, the inexact splitting approach is immediately applicable, by replacing (25) with a standard homogeneous Dirichlet problem.

Let us now consider the case of a genuine Navier-Stokes nonlinear problem faced with an implicit time discretization. For the sake of clarity, we refer to the implicit Euler discretization, even if the same approach can be adopted with every implicit time advancing scheme. In this case, the inexact splitting can be adopted in a fixed point iterative framework. More precisely, let us set $\mathbf{u}_{(0)}^{n+1} = \mathbf{u}^n$. Now, we solve the following problems for $k = 1, 2, \dots$

1. Steady Neumann problems (4).
2. Unsteady Neumann homogeneous problem: find $\mathbf{s}_{(k+1)}^{n+1}, \xi_{(k+1)}^{n+1}$ such that

$$\begin{cases} \left(\frac{\mathbf{s}_{(k+1)}^{n+1} - \mathbf{s}^n}{\Delta t}, \mathbf{v} \right) + \left((\mathbf{u}_{(k)}^{n+1} \cdot \nabla) \mathbf{s}_{(k+1)}^{n+1}, \mathbf{v} \right) + a(\mathbf{s}_{(k+1)}^{n+1}, \mathbf{v}) + \\ + b(\mathbf{v}, \xi_{(k+1)}^{n+1}) = (\mathbf{f}^{n+1}, \mathbf{v}) \\ b(\mathbf{s}_{(k+1)}^{n+1}, q) = 0, \end{cases} \quad (26)$$

3. Linear system:

$$\mathbf{B}\boldsymbol{\eta}_{(k+1)}^{n+1} = \mathbf{F}^{n+1} - \mathbf{S}_{(k+1)}^{n+1} \quad (27)$$

4. Homogeneous Dirichlet problem: as for problem (8), solve:

$$\left\{ \begin{array}{l} \left(\frac{\mathbf{e}_{(k+1)}^{n+1} - \mathbf{e}^n}{\Delta t}, \mathbf{v} \right) + \left((\mathbf{u}_{(k)}^{n+1} \cdot \nabla) \mathbf{e}_{(k+1)}^{n+1}, \mathbf{v} \right) + a \left(\mathbf{e}_{(k+1)}^{n+1}, \mathbf{v} \right) + \\ + b \left(\mathbf{v}, \varepsilon_{(k+1)}^{n+1} \right) = - \sum_{j=1}^m \frac{\eta_{j,(k+1)}^{n+1} - \eta_j^n}{\Delta t} (\mathbf{w}_j, \mathbf{v}) + \\ - \sum_{j=1}^m \eta_{j,(k+1)}^{n+1} \left((\mathbf{u}_{(k)}^{n+1} \cdot \nabla) \mathbf{w}_j, \mathbf{v} \right) \\ b \left(\mathbf{e}_{(k+1)}^{n+1}, q \right) = 0 \end{array} \right. \quad (28)$$

5. Final assembling: for θ real parameter, set:

$$\mathbf{u}_{(k+1)}^{n+1} = \theta \left(\mathbf{e}_{(k+1)} + \mathbf{s}_{(k+1)} + \sum_{j=1}^m \eta_{j,(k+1)} \mathbf{w}_j \right) + (1 - \theta) \mathbf{u}_{(k)}^{n+1}$$

The loop continues up to the fulfillment of a given stopping criterion.

Numerical evidence suggests that with an appropriate selection of the relaxation parameter θ , this algorithm converges in a few iterations to the fixed point, yielding the desired approximate solution of the augmented problem with an implicit time advancing scheme.

6 Numerical results

6.1 2D analytical cases

In the first set of simulations we aim at analyzing the algorithm proposed in Section 5 (with $\beta = \mathbf{u}$ and with a semi-implicit treatment of the convective term if not specified differently) on analytical test cases. We used the 2D Finite Elements code *Freefem++* (see www.freefem.org). These simulations have got also the aim of showing that the proposed algorithm could be implemented even with a standard (even commercial) finite element package.

6.1.1 Poiseuille flow

We simulate a flow in a rectangular domain Ω , whose size is $6 \times 1 \text{ cm}$, with a prescribed steady flow rate at the inlet ($F = 0.1 \text{ cm}^2/\text{s}$). Moreover, we set $\mu = 0.035 \text{ cm}^2/\text{s}$. As expected (see Remark 3.1), we recover the exact Poiseuille profile up to the discretization errors (see Figure 2).

Then, we solved the Navier-Stokes problem by using the implicit Euler scheme following the iterative procedure proposed in Section 5 for the treatment of the convective term. In Table 1 the mean number of subiterations per time step is shown. The convergence of the scheme can be strongly improved by an appropriate selection of θ .

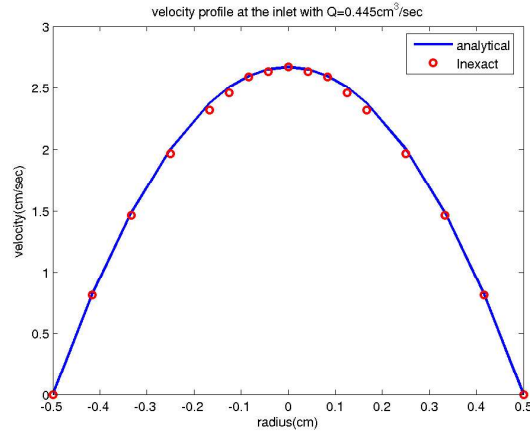


Figure 2: Comparison between the Poiseuille analytical solution and the inexact splitting computation. The solutions coincide up to the discretization error.

	$\theta = 0.1$	$\theta = 0.5$	$\theta = 0.9$
# subiterations	70	13	5

Table 1: Mean number of subiterations per time step using the implicit scheme for the treatment of the convective term for different values of θ

6.1.2 Womersley flow

In Figure 3 we illustrate the results obtained by prescribing a sinusoidal-in-time flow ($F(t) = 0.1 \cdot \cos(2\pi t) \text{ cm}^2/\text{s}$) at the inlet Γ of Ω . In this case we highlight the difference between the solutions obtained with the exact and the inexact splitting. In particular, as expected from the analysis of Section 3.1, we observe that the error significantly reduces far away from the boundary Γ , as pointed out also in Figure 5 and 4. Moreover, Figure 4 highlights that the error is proportional to the measure of Γ , as expected from the error analysis.

In practice, an affordable approach consists of enlarging the computational domain in order to confine the boundary error induced by the inexact splitting out of the region of interest. However, we point out that a small increase of the computational domain is enough. As a matter of fact, in our case it is sufficient to increase the length of the domain of 1 cm . Using the inexact splitting scheme the extension of the domain is smaller than the one required by the engineering approach (1 cm vs. $3\text{--}4 \text{ cm}$). Moreover, Table 2 confirms that the computational effort of the inexact splitting in the expanded domain is still small in comparison with the one request by the exact solver on the original domain Ω .

In Figure 6 the error of the inexact splitting for different values of the time step is shown. We notice that the boundary error does not depend on the time step. Moreover, in Figure 7 and 8 the dependence of the error on the fluid

viscosity and on the Womersley number respectively is shown. We notice that the smaller the viscosity (i.e. the bigger the Womersley number), the bigger is the error near the boundary. This is confirmed by the fact that increasing the pulsatility (i.e. the Womersley number) the error in solving equation (8) instead of (7) should increase.

Figure 9 shows that the boundary error does not depend on the spatial discretization step, as expected. Finally, in Figure 10 the pressure solution and the pressure error are shown with $\Delta t = 0.01s$ (left) and $\Delta t = 0.005s$ (right), pointing out that also the pressure error is localized near the boundary, independently of the discretization.

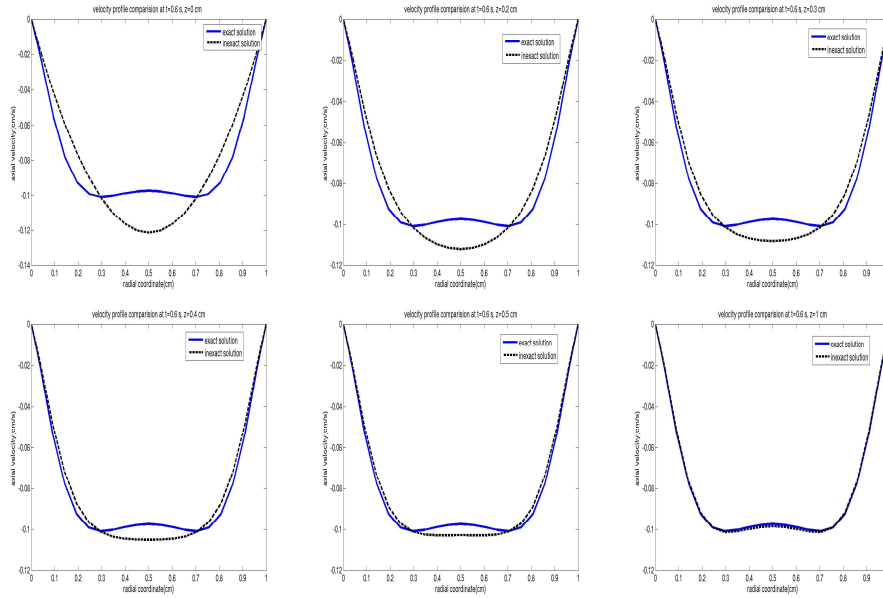


Figure 3: Womersley test case. Comparison between the solution computed by the exact Lagrangian multiplier solver (blue line) and the inexact splitting solution (red line) in the Womersley test case. The difference between the two solutions reduces when the distance from the boundary increases. (Top, left: distance=0cm; Top, middle: 0.2cm; Top, right: 0.3cm; Bottom, left 0.4cm; Bottom, middle: 0.5cm; Bottom, right: 1cm).

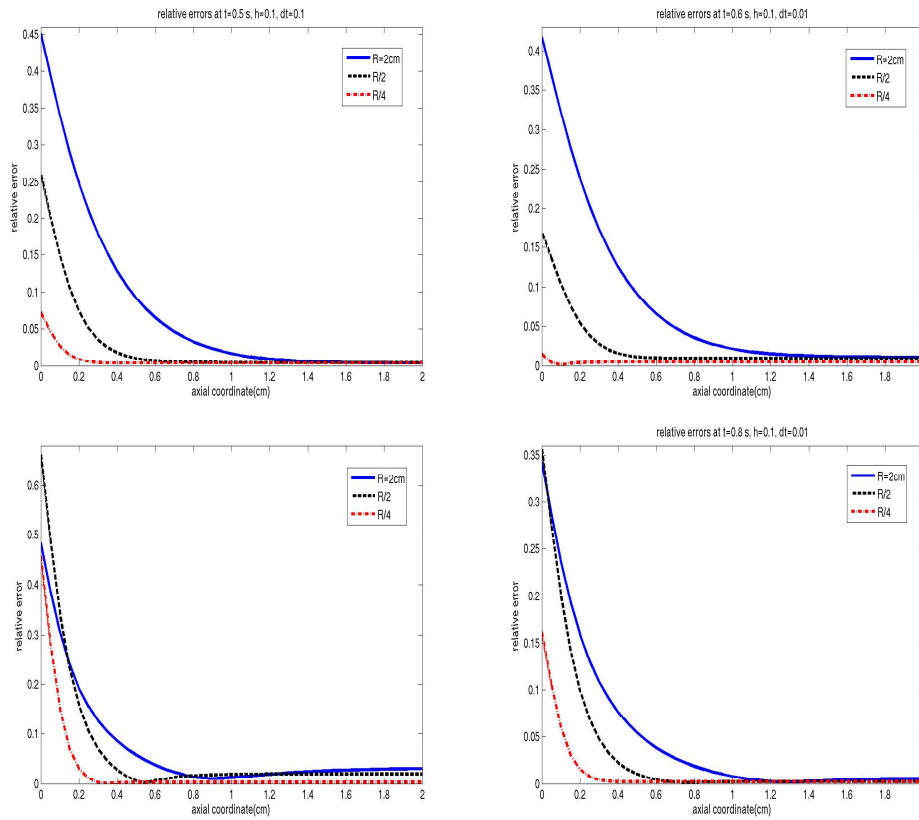


Figure 4: Womersley test case. Errors along the axial coordinate at different instants for different values of the pipe radius.

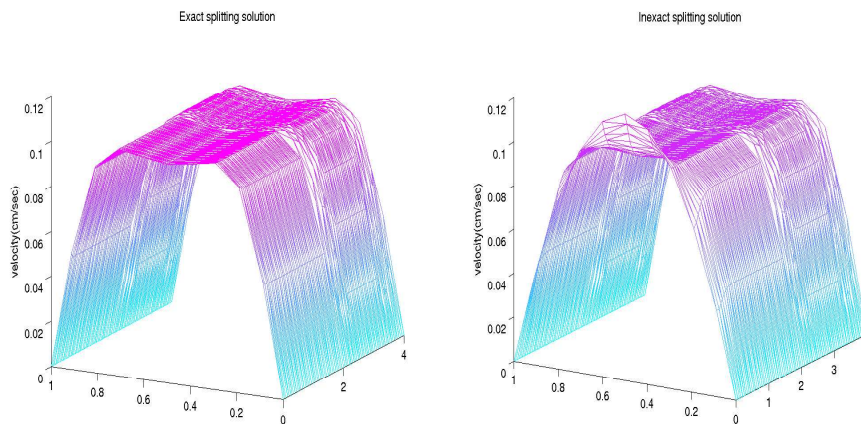


Figure 5: Womersley test case. Comparison between the velocity fields computed by the exact (left) and inexact (right) solvers.

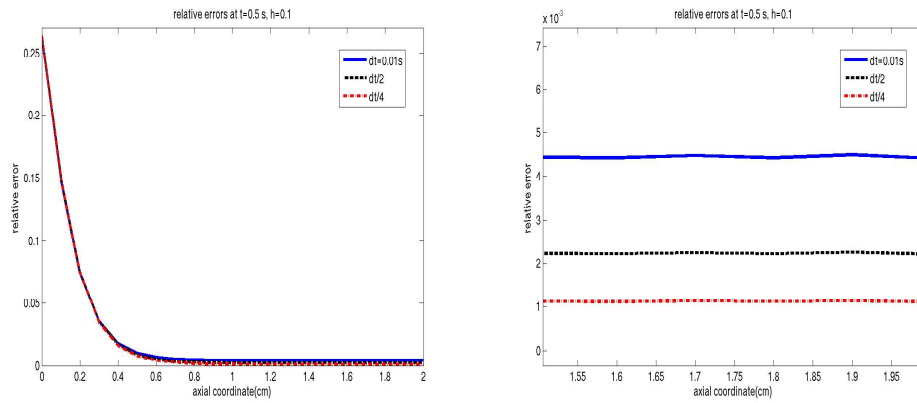


Figure 6: Womersley test case. Errors of the inexact splitting solution for different values of the time steps. On the right a detail of the errors in the centre of the domain, where the error is essentially due to the time discretization.

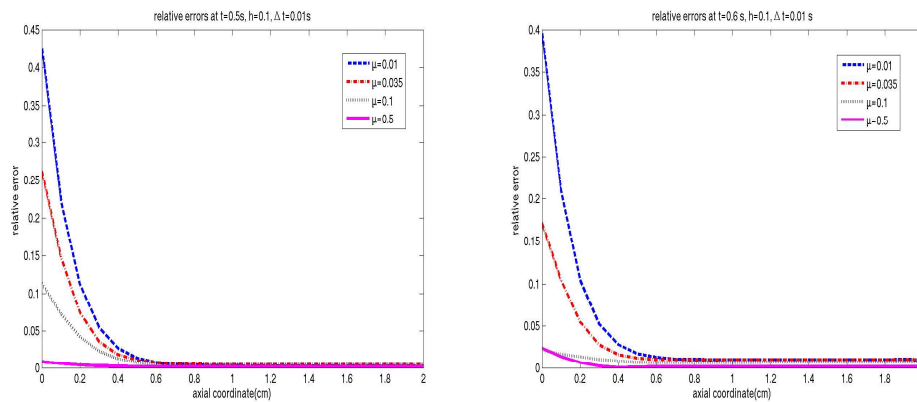


Figure 7: Womersley test case. Dependence of the error on the fluid viscosity.

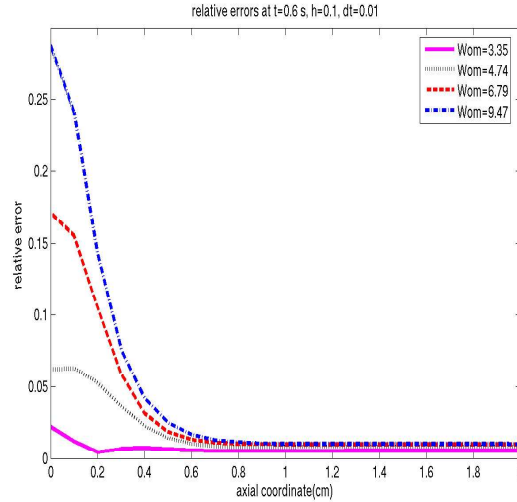


Figure 8: Womersley test case. Dependence of the error on the Womersley number.

6.2 2D realistic case

We focus our attention on a more realistic case. In particular, we simulate the flow of the fluid in an anastomosis of a by-pass (see Figure 12, left), whose sections have measure equal to 1cm and whose length is equal to 10cm . We prescribed the physiological flux shown in Figure 11 (right) both at the bottom and at the top inlet (with $50\text{cm}^2/\text{s}$ and $25\text{cm}^2/\text{s}$ as peak value respectively). Figure 11 (left) and Figure 12 show that the error is localized near the boundaries. Figure 13 points out again the dependence of the boundary error on the measure of Γ . Moreover, in Figure 14 the pressure field (left) and the pressure error (right) are shown.

In order to have a comparison between the computational efforts of the exact and inexact algorithms, we use again the latter in a domain extended of 0.5cm . Nevertheless, the CPU time (see Table 2) is about one half of the one requested by the GMRes-based solver when the flow rate is prescribed at one inlet. The CPU time reduction is even more evident when the flow rates are prescribed on both the inlets. Therefore, differently from the GMRes algorithm, the computational effort of the proposed algorithm does not depend on the number of the section where we prescribe the flow rate.

6.3 3D computations

In the second set of simulations we studied the efficiency of the proposed algorithm for 3D simulations, using the 3D Finite Element Library *Lifev* (see www.lifev.org).

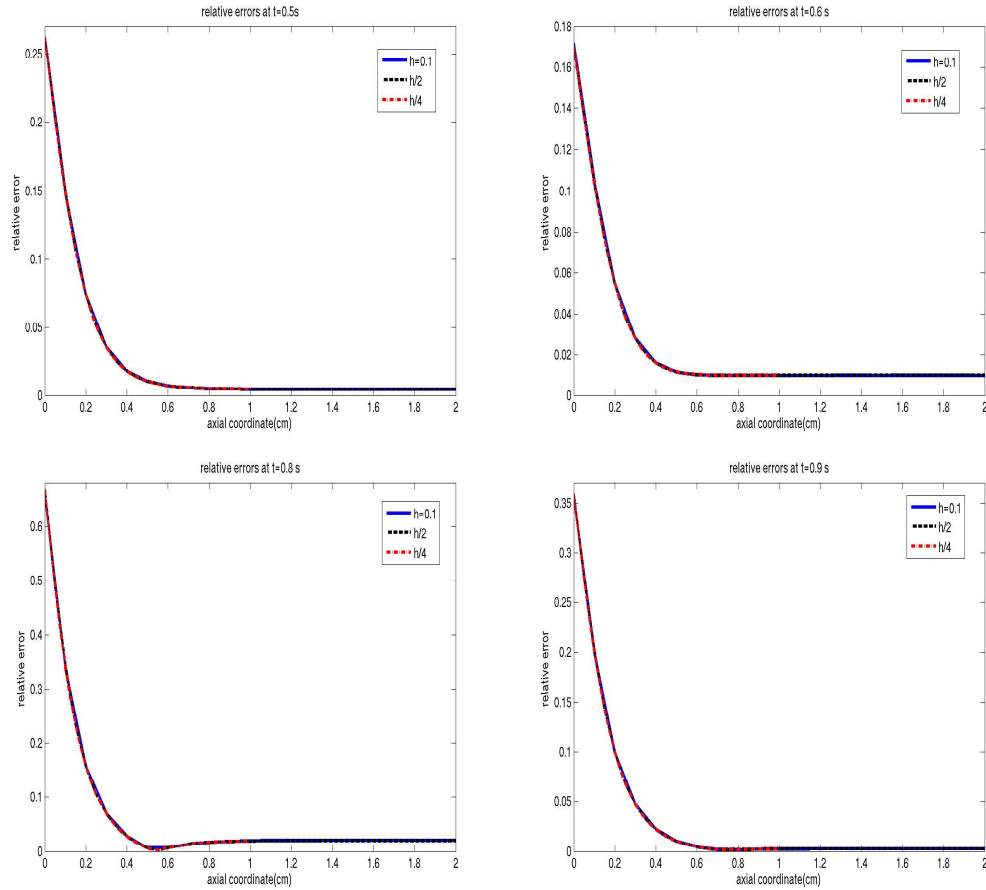


Figure 9: Womersley test case. Dependence of the error on the space discretization.

6.3.1 An analytical test case

We simulate the flow of the fluid in a cylinder with radius $r = 1\text{cm}$ and length $l = 5\text{cm}$ by prescribing a sinusoidal-in-time flow ($F(t) = 0.1 \cdot \cos(2\pi t)\text{cm}^3/\text{s}$) at the inlet. In Figure 15 the error with the solution obtained with the exact algorithm is shown for different spatial discretization steps. As for the 2D case, the error is confined in the neighborhood of the boundary. Figure 16 shows the axial velocity obtained with the exact (left) and with the inexact (right) algorithm.

6.3.2 Carotid

Finally, we apply the proposed algorithm in a carotid domain obtained from real data of a patient through a cast produced by D. Liepsch - FH Munich. We impose physiological flow rates similar to the one in Figure 11 (right) at both

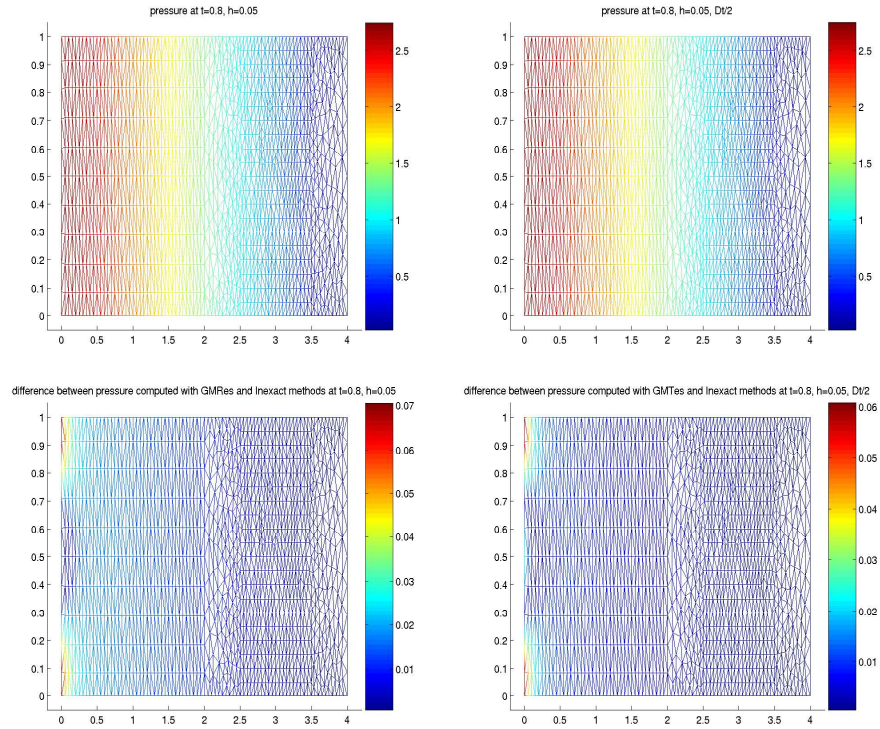


Figure 10: Womersley test case. Top: Pressure solution with $\Delta t = 0.01s$ (left) and $\Delta t = 0.005s$ (right). Bottom: Pressure splitting error. The time steps is the same of the pictures at the top.

the outlets of the domain. In Figure 17 the velocity fields obtained with the inexact (up) and with the exact (bottom) algorithm are shown. Also in this case it is evident that the error is confined near the boundary.

Acknowledgments

Numerical results of this work have been obtained with the finite element codes LifeV (developed at MOX - Dipartimento di Matematica - Politecnico di Milano, at EPFL in Lausanne and at INRIA at Paris, see www.lifev.org). The authors gratefully acknowledge M. Prosi who provided the bifurcation computational domain and all the LifeV staff.

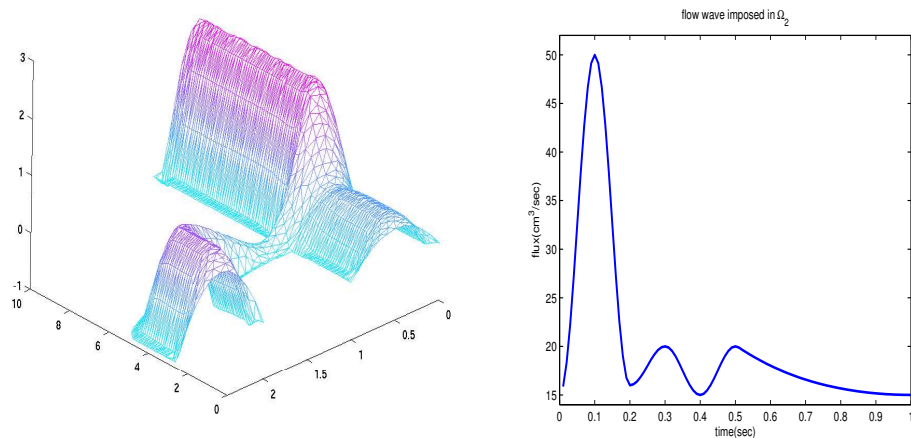


Figure 11: Anastomosis solution and physiological flux imposed at the two inlets

Test Case	Exact Splitting	Inexact Splitting	CPU t.in./ CPU t.ex.
Womersley	10min 31s	5min 46s	0.55
Anastomosis $m = 1$	7min 58s	4min 27s	0.56
Anastomosis $m = 2$	11min 3s	4min 33s	0.41

Table 2: CPU times for the two cases illustrated. In the Womersley test case the final time was 2s, in the anastomosis one it was 1s, using for both the simulations $\Delta t = 0.01s$. The inexact splitting computations have been performed on an extended domain, so that the two solutions in the domain of interest covered by the exact solver coincide up to the discretization errors.

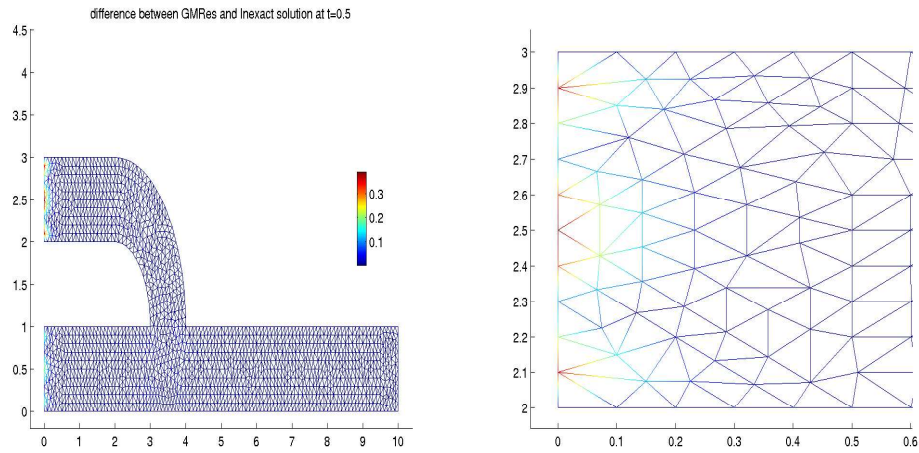


Figure 12: Solution in the anastomosis case: velocity splitting error. On the right a zoom of the figure on the upper inlet.

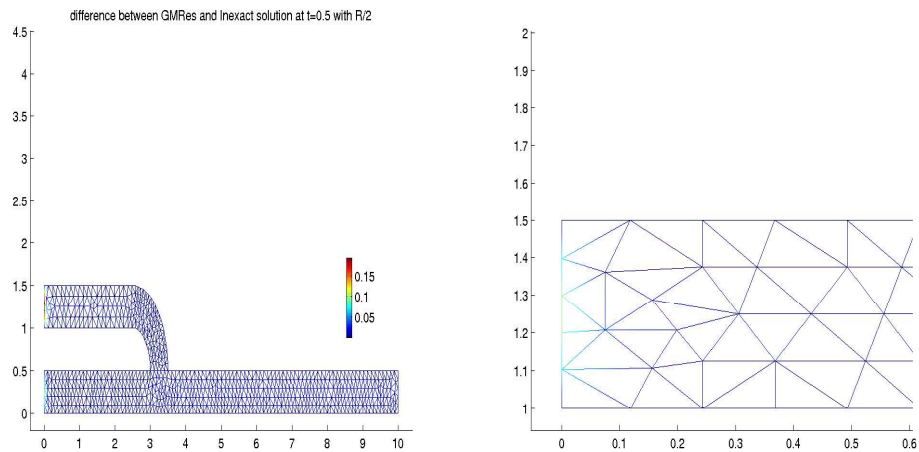


Figure 13: The same as in Figure 12 with an inlet radius one half of the case plotted above.

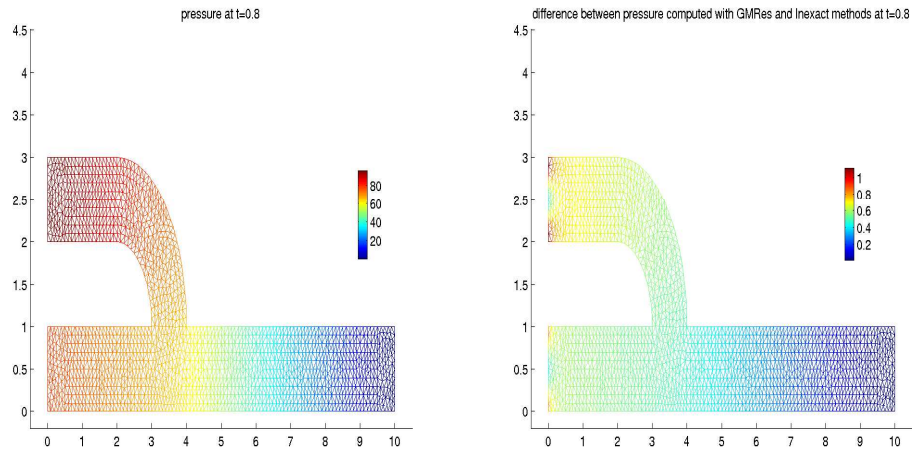


Figure 14: Pressure solution (left) and difference between exact and inexact splitting solutions (right) for the anastomosis computation.

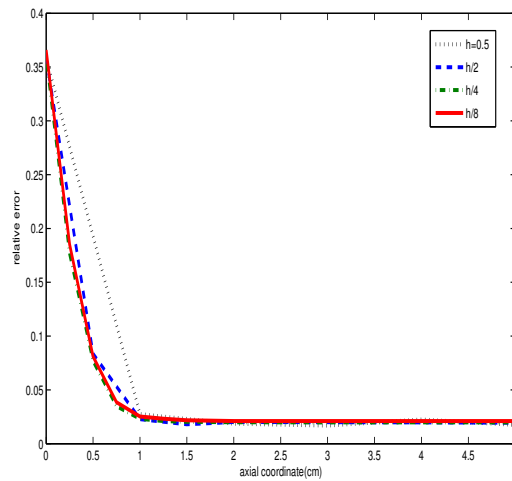


Figure 15: Computations in 3D: relative error for the Womersley solutions in the cylinder for different values of h , $\Delta t = 0.01s$.

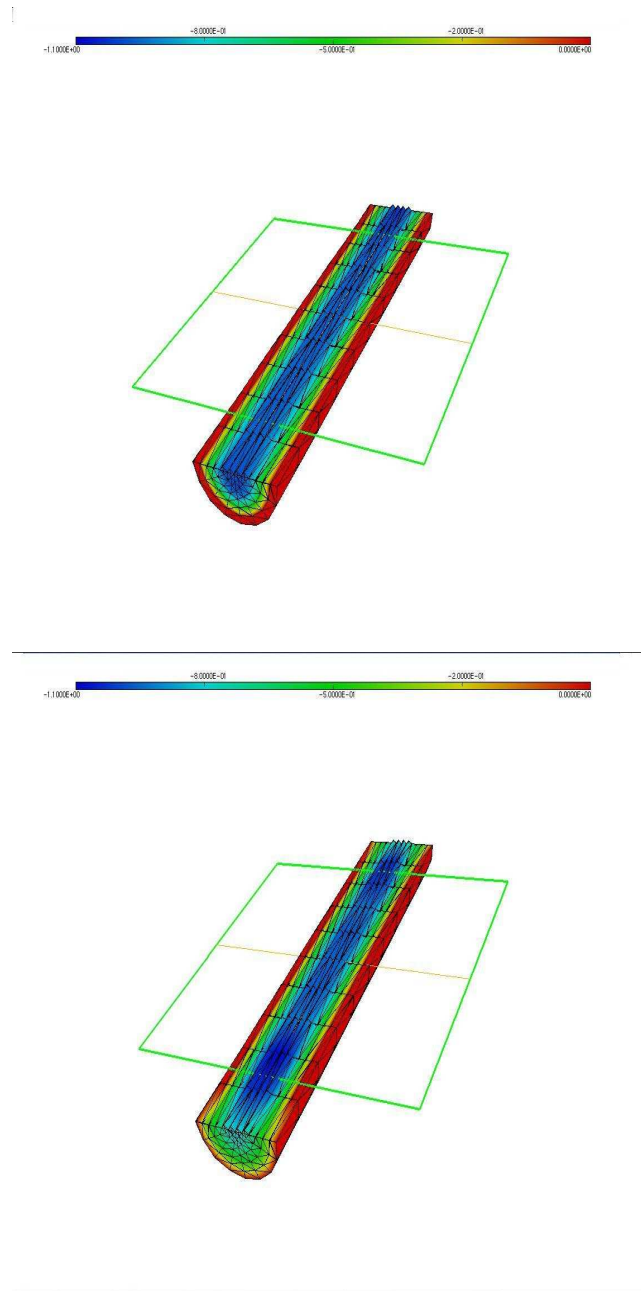


Figure 16: Computations in 3D, Womersley solutions: comparison between the solutions obtained with the exact (left) and the inexact (right) algorithm, $t=0.9\text{sec}$

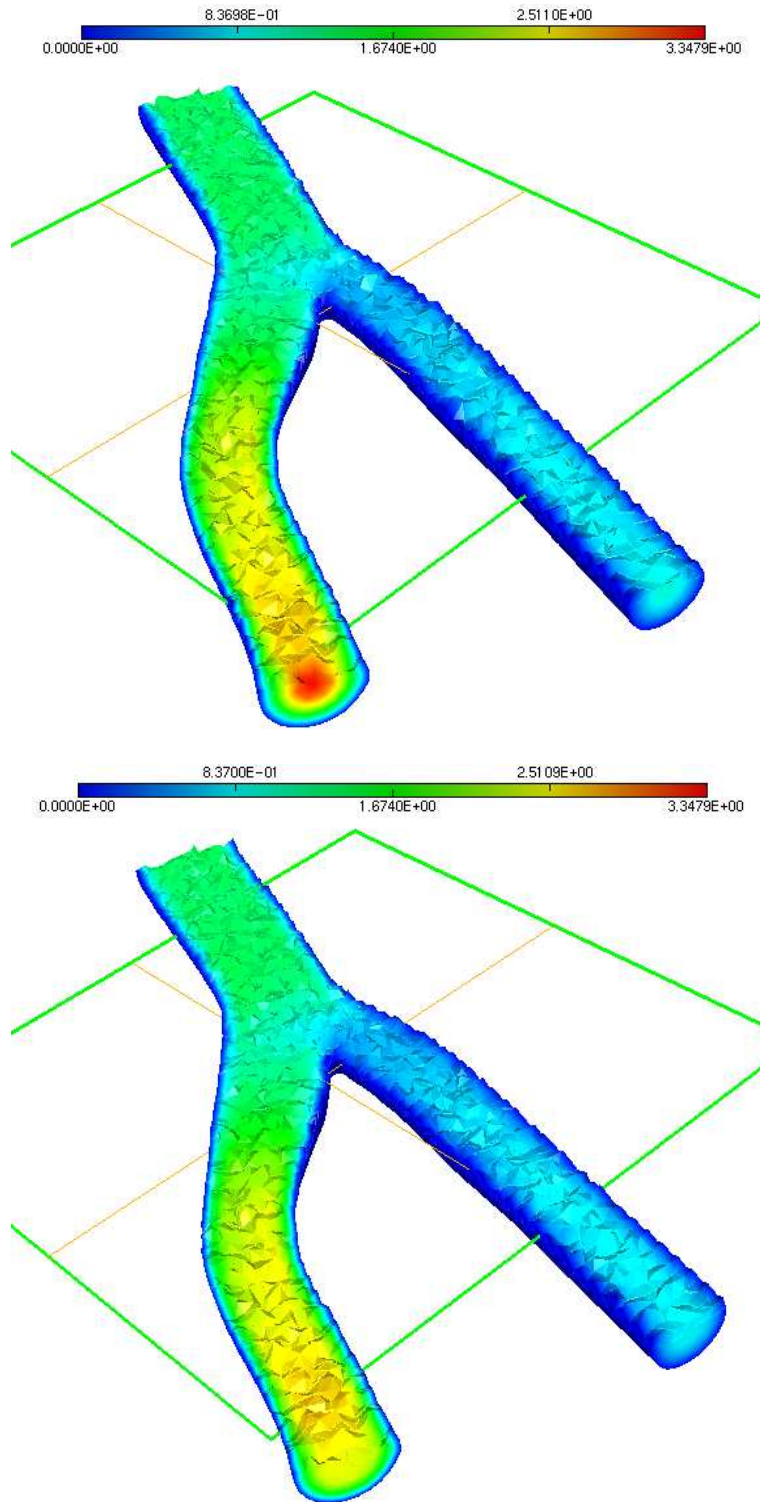


Figure 17: Computations in 3D: carotid solution. Velocity with inexact (up) and with exact (bottom) algorithm, $t=0.13s$

References

- [1] L. Formaggia, J. F. Gerbeau, F. Nobile, and A. Quarteroni. On the coupling of 3d and 1d navier-stokes equations for flow problems in compliant vessels. *Comp.Math. Appl. Mech. Eng.*, 191:561–582, 2001.
- [2] L. Formaggia, J. F. Gerbeau, F. Nobile, and A. Quarteroni. Numerical treatment of defective boundary conditions for the navier-stokes equation. *SIAM J Num Anal*, 40(1):376–401, 2002.
- [3] L. Formaggia, F. Nobile, A. Quarteroni, and A. Veneziani. Multiscale modelling of the circulatory system: a preliminary analysis. *Computing and Visualisation in Science*, 2:75–83, 1999.
- [4] L. Formaggia and A. Quarteroni. Mathematical modelling and numerical simulation of the cardiovascular system. In *Modelling of Living System, Ayache N., Ciarlet P.G., Lions J.L. (eds). Handbook of Numerical Analysis.* Elsevier, Amsterdam, 2003.
- [5] L. Formaggia and A. Veneziani. Reduced and multiscale models for the human cardiovascular system. In *Lecture Notes, VKI Lecture Series 2003.* Brussels.
- [6] P. Girault and V. Raviart. *Navier-Stokes equations.* Springer, 1986.
- [7] J.G. Heywood, R. Rannacher, and S. Turek. Artificial Boundaries and Flux and Pressure Conditions for the Incompressible Navier–Stokes Equations. *International Journal for Numerical Methods in Fluids*, 22:325–352, 1996.
- [8] A. Quarteroni and A. Valli. *Numerical Approximation of Partial Differential Equations.* Springer, 1994.
- [9] R. Rannacher. On chorin’s projection method for the incompressible navier-stokes equations. In *Lecture Notes.* Springer, 1991.
- [10] Y. Saad. *Iterative Methods for Sparse Linear System.* PWS Publishing Company, Boston, 1996.
- [11] A. Veneziani. Boundary conditions for blood flow problems. In F. Brezzi et al., editor, *Proc. of ENUMATH97*, pages 596–605. World Scientific, 1998.
- [12] A. Veneziani and C. Vergara. Flow rate defective boundary conditions in haemodynamics simulations. *Int J Num Meth Fluids*, 47:803–816, 2005.